Journal of New Results in Science

https://dergipark.org.tr/en/pub/jnrs

Research Article

Open Access

E-ISSN:1304-7981 https://doi.org/10.54187/jnrs.1568210

Investigation of W, Pb, and Bi elements from neutron shielding point of view

Yasin Gaylan[1]

Keywords:
Al-(W-Pb-Bi) composites,
Neutron shielding,
Gamma-ray shielding,
Monte Carlo simulation

Abstract – This study investigates the performances of tungsten, lead, and bismuth elements, which are widely used for shielding gamma-ray, from the neutron shielding point of view using the Monte Carlo N-Particle (MCNP6.2) simulation code. The study analyzed the neutron shielding capacities of Al matrix composites containing 30% W, Pb, and Bi. In addition, the shielding properties of secondary gamma-ray with an energy of 0.478 MeV resulting from neutron-boron interaction were also investigated. The results show that for thermal and intermediate energy neutrons, Al-30%W composite gives very good results by separating from Al-30%Pb and Al-30%Bi composites. However, Al-%30Pb and Al-%30Bi composites are also effective for fast neutrons. Regarding the gamma-ray, it was calculated that the Al-30%Pb composite exhibited the highest shielding performance. These findings provide important data on the contribution of W, Pb, and Bi elements used as gamma-ray shielding to neutron shielding in different neutron energy ranges and reveal that these elements should be used strategically with appropriate combinations depending on the neutron energy in neutron shielding designs.

1. Introduction

Neutrons interact with matter and perform scattering or absorption reactions depending on their energy. In neutron shielding, elements with high scattering or absorption cross-sections are preferred depending on the energy of the incident neutron. While light elements are used to reduce the energy of fast neutrons to the thermal energy level, neutrons slowed down to the thermal level are absorbed by elements with high neutron absorption cross-sections. During these scattering and absorption reactions, secondary gamma rays are produced by interacting neutrons with matter. An effective neutron shielding should slow down fast neutrons, absorb slow neutrons, and shield the secondary gamma-ray generated during these reactions.

In literature, Boron (B), Gadolinium (Gd), and Samarium (Sm) elements are widely used as neutron shielding. Boron produces secondary gamma-rays with an energy of 0.478 MeV in the neutron absorption reaction, while Gd produces high-energy gamma-rays on a broader energy range [1,2]. To shield these emitted secondary gamma rays, researchers have been developing neutron shields with elements such as tungsten (W), lead (Pb), and bismuth (Bi) [3–5]. For example, Cong et al. doped tungsten into the Al-Gd_2O_3 composite they developed to shield thermal neutrons and secondary gamma-rays emitted from neutron interactions [1]. Another study investigated the ideal mixing ratio of Gd_2O_3-W composite regarding neutron macroscopic cross-section (MaCS) and gamma-ray lineer attenuation coefficient (LAC) [6]. In glass-based neutron shielding, lead and bismuth have increased the gamma-ray LAC of glasses [3,7]. Similar elements are also preferred in polymer-based neutron shielding to shield gamma rays [8,9].

[1]yasingaylan@gmail.com (Corresponding Author)
[1]Department of Metallurgical and Materials Engineering, Zonguldak Bülent Ecevit University, Zonguldak, Türkiye
Article History: Received: 16 Oct 2024 — Accepted: 19 Dec 2024 — Published: 31 Dec 2024

This study investigated the contributions of W, Pb, and Bi elements in neutron shielding and secondary gamma-ray. For this purpose, the neutron MaCS and attenuation rates of Al-30% (W, Pb, Bi) composites were calculated for thermal, intermediate, and fast neutrons using the MCNP6.2 simulation code. In addition, the shielding properties of secondary gamma-ray produced by neutron-boron interaction were investigated and compared.

2. Material and Methods

The Monte Carlo N-Particle (MCNP) simulation code is a versatile tool widely used in the fields of nuclear science and engineering to model radiation transport and its interactions with matter. Developed by Los Alamos National Laboratory, the MCNP simulation code employs Monte Carlo methods to simulate the interactions of particles such as neutron, photon, and electron across a broad energy spectrum. MCNP facilitates the solution of complex problems in reactor physics, shielding design, medical physics, and radiation shielding [4,10–15]. With its high capacity to achieve strong agreement with experimental data, MCNP stands out as an essential tool for researchers working in the field of radiation transport simulations [16].

In this study, MCNP6.2 was used to calculate the thermal, intermediate, and fast neutron macroscopic cross-sections of Al-30%(W, Pb, Bi) composites, as well as the neutron attenuation rates for shields with thicknesses ranging from 0.5 cm to 5 cm. Additionally, the program was employed to determine the LAC for photons with an energy of 0.478 MeV and the photon attenuation rates for shields of the same thickness range.

Neutrons are classified according to their kinetic energy. There is no sharp distinction or energy limit between neutron classes; however, neutrons can be classified according to their energy as follows:

i. Thermal neutrons: 0.003 eV - 0.4 ev

ii. Intermediate neutrons: 100 eV-200 keV

iii. Fast neutrons: 200 keV-10 MeV

This study determined that the thermal neutron energy was 0.1 eV, the intermediate neutron energy was 1 keV, and the fast neutron energy was 1 MeV [17].

The simulation geometry shown in Figure 1 initially calculated the flux with no target material in place. Subsequently, the flux was measured by placing the target material between the neutron/gamma source and the detector. (2.1) calculated the gamma-ray, thermal, intermediate, and fast neutron attenuation rate. (2.2) and (2.3) were used to calculate the gamma-ray LAC and neutron MaCS using the Beer-Labmert law.

$$\text{Neutron/Gamma Attenuation Rate } (\%) = \left(1 - \frac{\mathrm{I_x}}{\mathrm{I_0}}\right) 100$$

$$I_x = I_o e^{-\Sigma_t x}$$

$$I_x = I_o e^{-\lambda x}$$

Where I_o and I_x represent the incoming and transmitted neutron-photon intensities, respectively, x is the absorber thickness in centimeters, $\sum_t$ is the neutron MaCS, and λ is the gamma-ray LAC of the absorber medium.

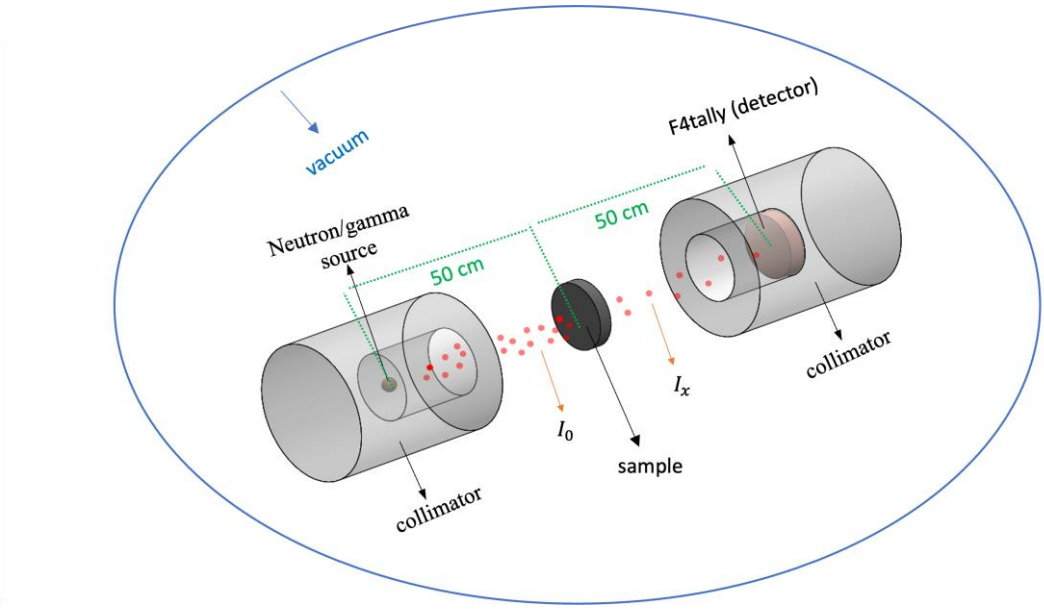

Figure 1. The geometry of the Monte Carlo simulation setup

3. Results and Discussion

Figures 2, 3, and 5 present the MCNP6.2 simulation results for thermal, intermediate, and fast neutron MaCS and attenuation rates as a function of thickness, ranging from 0.5 to 5 cm, for Al-30(W, Pb, and Bi) composites. Among these, the Al-30W composite demonstrates the highest neutron MaCS and attenuation ratio at the thermal energy level. At 5 cm thickness, the Al-30W composite attenuates 50.02% of thermal neutrons, whereas the Al-30Pb and Al-30Bi composites achieve attenuation rates of 44.88% and 42.65%, respectively. Tungsten doping is the most effective in enhancing the thermal neutron attenuation rate compared to lead and bismuth.

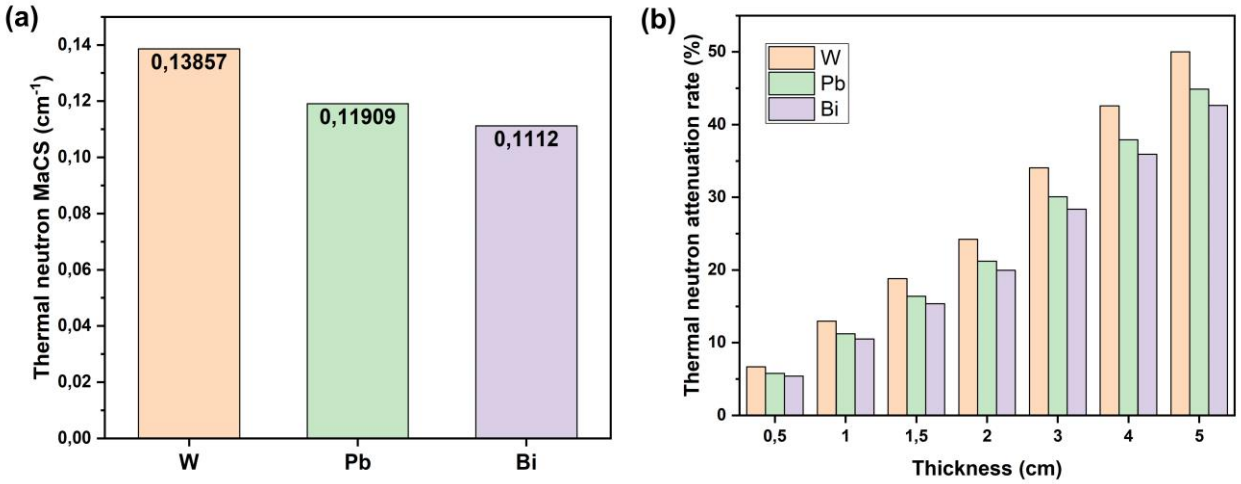

Figure 2. a) Thermal neutron macroscopic cross-section and b) Attenuation rate graph

For intermediate neutrons, the neutron MaCS values for Pb and Bi-doped composites decrease compared to thermal-energy neutrons. In contrast, the MaCS of the Al-30W composite increases significantly from 0.139 cm^{-1} for thermal neutrons to 0.242 cm^{-1} for intermediate neutrons. At a thickness of 3 cm, the intermediate neutron attenuation rate of the Al-30W composite is 51.61%, while those of the Al-30Pb and Al-30Bi composites are 27.72% and 28.10%, respectively. These intermediate-energy results align with the energy-dependent cross-section trends of W-184, Pb-208, and Bi as illustrated in Figure 4 [18].

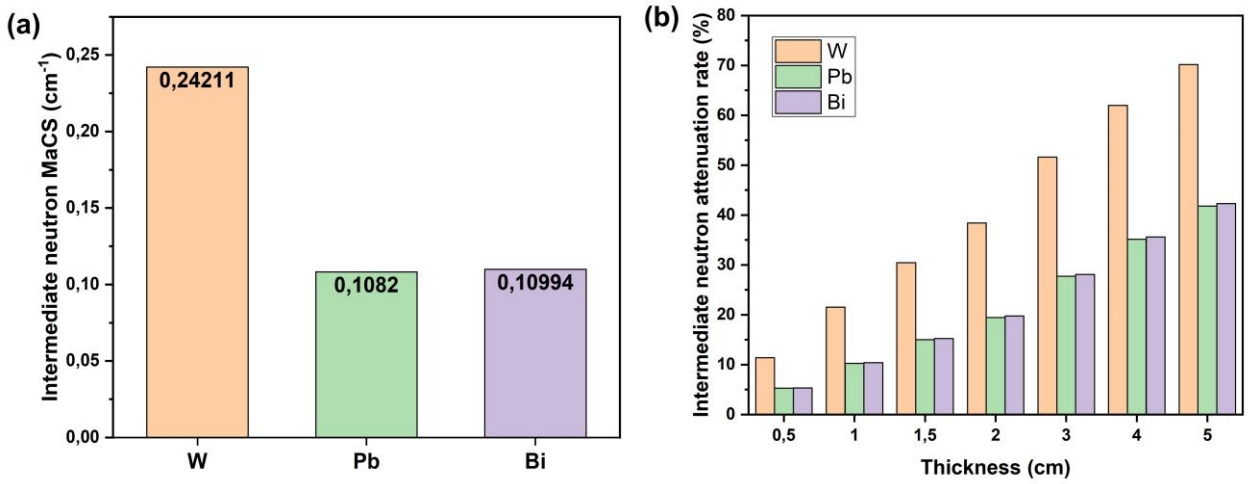

Figure 3. a) Intermediate neutron macroscopic cross-section and b) Attenuation rate graph

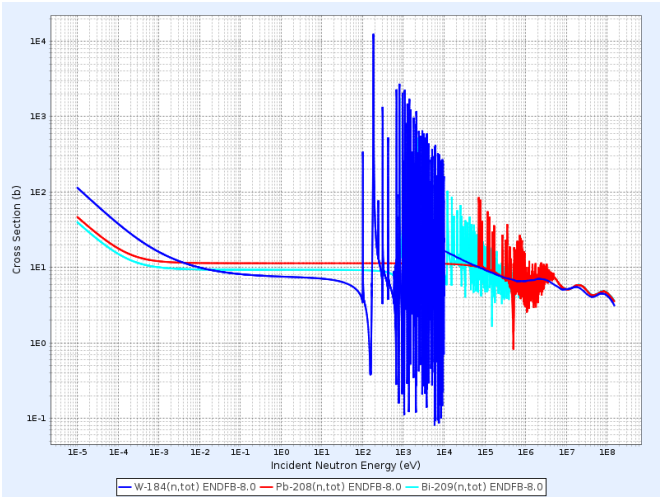

Figure 4. W, Pb, and Bi energy dependent cross-section plot

Compared to thermal neutrons, the MaCS of the Al-30W composite shows a 74% increase for intermediate-energy neutrons but decreases for fast neutrons. For fast neutrons, the MaCS of the Al-30W composite decreases to 0.158 cm^{-1}, whereas the MaCS values of the Al-30Pb and Al-30Bi composites increase to 0.145 cm^{-1} and 0.143 cm^{-1}, respectively. At 5 cm thickness the highest attenuation rate is 54.65% with Al-30W, while the attenuation rates of Al-30Pb and Al-30Bi are 51.56% and 51.07% respectively.

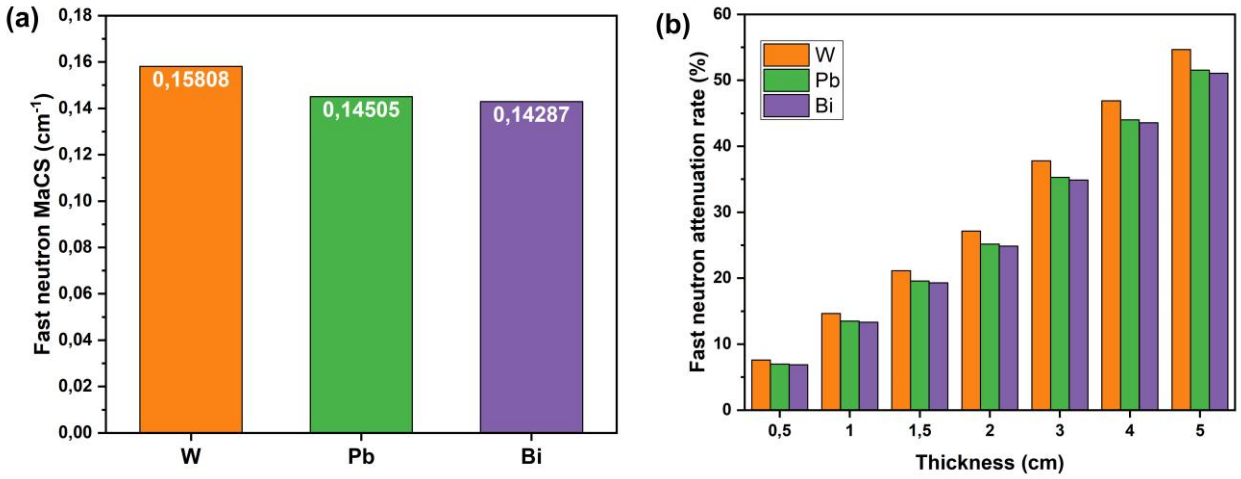

Figure 5. a) Fast neutron macroscopic cross-section and b) Attenuation rate graph

Figure 6 shows the LAC and photon attenuation rate plots of Al-30(W, Pb, and Bi) composites for photons with an energy of 0.478 MeV. The 0.478 MeV energy photons were chosen because they are the energy of secondary gamma-ray resulting from the interaction of thermal neutrons with boron, which has a high neutron absorption cross-section and is widely used in neutron shielding. The W doping provides better shielding than Pb and Bi for thermal, intermediate, and fast neutrons. It has the smallest LAC value and photon attenuation rate for photons with an energy of 0.478 MeV. For 0.478 MeV energy photons, the photon attenuation of W, Pb, and Bi-doped composites in a 2 cm thick shield was calculated as 52.92%, 54.09%, and 53.99%, respectively. Among these, the Al 30Pb composite was the most effective in gamma-ray shielding. Pb is highly effective in gamma-ray shielding due to its high atomic number and density, which enhance the likelihood of photoelectric interactions.

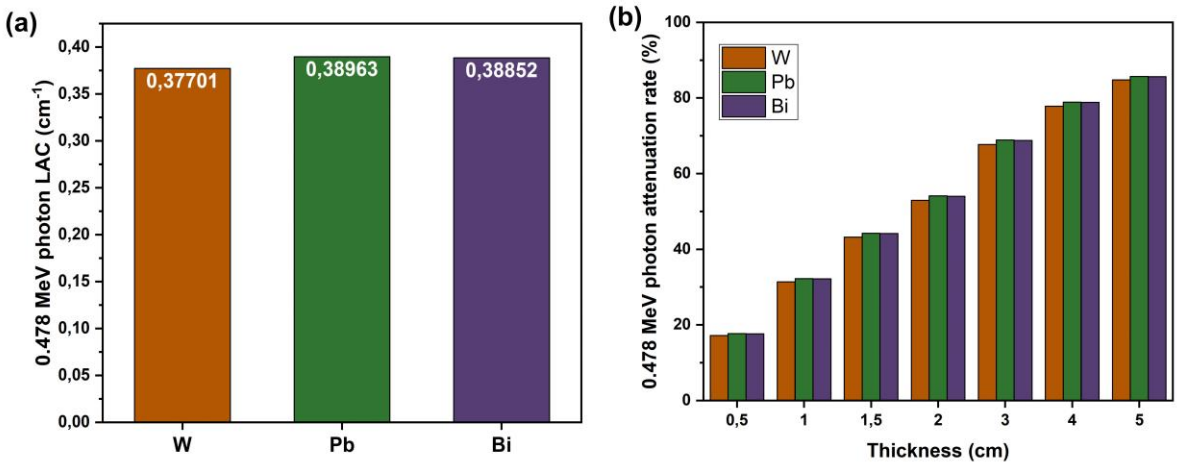

Figure 6. a) 0.478 MeV photon LAC and b) Attenuation rate graph

4. Conclusion

This study evaluated the neutron shielding performances of W, Pb, and Bi, commonly used for gamma-ray shielding, using the MCNP6.2 simulation code. MaCS and attenuation rate values were calculated for thermal, intermediate, and fast neutrons, as well as LAC values for photons with an energy of 0.478 MeV. For thermal neutrons, the Al-30%W composite demonstrated the highest neutron absorption performance. For intermediate-energy neutrons, the W-doped composite achieved an attenuation rate of 70.15% at a thickness of 5 cm due to its increased MaCS, highlighting W as the optimal element for shielding against intermediate-energy neutrons. Although W exhibited the highest attenuation rate for fast neutrons, the shielding performances of Pb- and Bi-doped composites were found to be comparable to that of the Al-30%W composite. In terms of gamma rays, the Al-30%Pb composite exhibited the highest LAC and attenuation ratio for photons with an energy of 0.478 MeV, whereas the Al-30%W composite demonstrated the lowest performance. However, considering W's superior neutron shielding capabilities, the 2–3% reduction in gamma-ray attenuation, depending on thickness, is within an acceptable range.

In conclusion, this study demonstrates the performance of W, Pb, and Bi in neutron and gamma-ray shielding. It shows that these elements should be used strategically according to the energy of the neutron to be shielded. In particular, it is concluded that W provides superior shielding for thermal and intermediate energy neutrons, while Pb is the most effective element for gamma-ray shielding. These findings suggest that the combinations of components in neutron shielding designs should be optimized depending on the neutron energy. In light of this study, the Al-30W-20B4C composite will be examined in our future study. The present study demonstrates that W enhances the neutron shielding performance of the Al-30W-20B_4C composite while also mitigating secondary gamma rays generated from boron-neutron interactions.

Author Contributions

The author read and approved the final version of the paper.

Conflict of Interest

The author declares no conflict of interest.

Ethical Review and Approval

No approval from the Board of Ethics is required.

References

[1] S. Cong, G. Ran, Y. Li, Y. Chen, *Ball-milling properties and sintering behavior of Al-based Gd2O3–W shielding materials used in spent-fuel storage*, Powder Technology 369 (2020) 127–136.

[2] J. Dumazert, R. Coulon, Q. Lecomte, G. H. V. Bertrand, M. Hamel, *Gadolinium for neutron detection in current nuclear instrumentation research: A review*, Nuclear Instruments and Methods in Physics Research, Section A: Accelerators, Spectrometers, Detectors and Associated Equipment 882 (2018) 53–68.

[3] Y. S. Rammah, I. O. Olarinoye, F. I. El-Agawany, A. El-Adawy, E. S. Yousef, *The f-factor, neutron, gamma radiation and proton shielding competences of glasses with Pb or Pb/Bi heavy elements for nuclear protection applications*, Ceramics International 46 (2020) 27163–27174.

[4] N. Ekinci, K. A. Mahmoud, S. Sarıtaş, B. Aygün, M. M. Hessien, I. Bilici, Y. S. Rammah, *Development of Tincal based polypropylene polymeric materials for radiation shielding applications: Experimental, theoretical, and Monte Carlo investigations*, Materials Science in Semiconductor Processing 146 (2022) 106696.

[5] Y. Wang, W. Xiao, J. Huang, S. Zou, J. Liu, Z. Ren, S. Liu, Y. Liu, Y. Huang, *Microstructure, mechanical and corrosion property of neutron and γ-ray shielding (Gd2O3+W)/Al composites*, Ceramics International 50 (2024) 41448–41460.

[6] Y. Gaylan, A. Bozkurt, *Investigating Thermal Neutron and Gamma Ray Shielding Properties of Al Matrix Gd2O3-and W-Doped Composites Using Monte Carlo Simulations*, Süleyman Demirel University Faculty of Arts and Science Journal of Science 19 (2024) 75–85.

[7] E. Salama, A. Maher, G. M. Youssef, *Gamma radiation and neutron shielding properties of transparent alkali borosilicate glass containing lead*, Journal of Physics and Chemistry of Solids 131 (2019) 139–147.

[8] F. Akman, H. Ozdogan, O. Kilicoglu, H. Ogul, O. Agar, M. R. Kacal, H. Polat, A. Tursucu, *Gamma, charged particle and neutron radiation shielding capacities of ternary composites having polyester/barite/tungsten boride*, Radiation Physics and Chemistry 212 (2023) 111120.

[9] Q. Shao, Q. Zhu, Y. Wang, S. Kuang, J. Bao, S. Liu, *Development and application analysis of high-energy neutron radiation shielding materials from tungsten boron polyethylene*, Nuclear Engineering and Technology 56 (2024) 2153–2162.

[10] K. Schweda, D. Schmidt, *Improved response function calculations for scintillation detectors using an extended version of the MCNP code*, Nuclear Instruments and Methods in Physics Research Section A: Accelerators, Spectrometers, Detectors and Associated Equipment 476 (2002) 155–159.

[11] R. Taghavi, H. R. Mirzaei, S. M. R. Aghamiri, P. Hajian, *Calculating the absorbed dose by thyroid in breast cancer radiotherapy using MCNP-4C code*, Radiation Physics and Chemistry 130 (2017) 12–14.

[12] R. G. Abrefah, R. B. M. Sogbadji, E. Ampomah-Amoako, S. A. Birikorang, H. C. Odoi, B. J. B. Nyarko, *Design of boron carbide-shielded irradiation channel of the outer irradiation channel of the Ghana Research Reactor-1 using MCNP*, Applied Radiation and Isotopes 69 (2011) 85–89.

[13] M. H. A. Mhareb, Y. S. M. Alajerami, M. I. Sayyed, K. A. Mahmoud, T. Ghrib, M. K. Hamad, Q. A. Drmosh, N. Sfina, M. A. Almessiere, *Morphological, optical, structural, mechanical, and radiation-shielding properties of borosilicate glass–ceramic system*, Ceramics International 48 (2022) 35227–35236.

[14] C. Kursun, M. Gao, A. O. Yalcin, K. A. Parrey, Y. Gaylan, *Structure, mechanical, and neutron radiation shielding characteristics of mechanically milled nanostructured (100-x)Al-xGd2O3 metal composites*, Ceramics International 50 (2024) 27154–27164.

[15] X. Lian, W. Xu, P. Zhang, W. Wang, L. Xie, X. Chen, *Design and mechanical properties of SiC reinforced Gd2O3/6061Al neutron shielding composites*, Ceramics International 49 (2023) 27707–27715.

[16] H. Ghninou, A. Gruel, A. Lyoussi, C. Reynard-Carette, C. El Younoussi, B. El Bakkari, Y. Boulaich, *Evaluation of the CNESTEN's TRIGA Mark II research reactor physical parameters with TRIPOLI-4® and MCNP*, Nuclear Engineering and Technology 55 (2023) 4447–4464.

[17] M. F. L'Annunziata, *Radioactivity: Introduction and History, From the Quantum to Quarks: Second Edition*, Elsevier Inc., 2016.

[18] *Nuclear Data Center at KAERI*, https://atom.kaeri.re.kr/, Accessed 9 Dec 2024